

# SITE TEST OF SYNCHRONOUS STARTING AT MIDONO PUMPING-UP POWER STATION, TOKYO ELECTRIC POWER CO., INC.

Mitsuru Takahashi

Kawasaki Factory

Sadao Kambara

Electric Power Engineering Dept.

## I. INTRODUCTION

The Midono power station is a part of the Azusagawa Development which produces an overall output of 900,000 kW. It is a pumping-up station with a maximum output of 245,000 kW and is equipped with 2 units for generation only and 2 units which can also be used for pumping.

In this station, the synchronous starting method was applied for generator/motor start when pumping up operation start. Examples of this method can not be seen either in Japan or abroad and the results of this system deserve attention.

The results of synchronous starting site tests were not only completely successful in all respects but we also obtained a lot of valuable data for future application of the synchronous starting method. This article will describe the synchronous starting method for use in pumping-up power stations mainly on the basis of these test results, and we hope that it will serve as a reference for all concerned.

The main points from the test results are as follows.

- 1) The excitation ratio of the generator and generator/motor was changed in respect to the possible synchronization limit region during the initial starting period and the distinct characteristics of the region were obtained.
- 2) The possible starting region during acceleration up to the rated speed was confirmed and the relation between the turbine torque and the excitation product of the two units was obtained.
- 3) It was possible to perform smooth and accurate switching to the direct-coupled exciter from the separate excitation equipment and also shifting to AVR and APFR operation from constant excitation.
- 4) Stable operation of all parts from synchronization to the line until pumping-up operation was confirmed.
- 5) The starting test in water was conducted without using water depression equipment in the pump turbine and the set was successfully speeded up to synchronization and operated to pumping-up. The possible starting region was also confirmed in respect to the increase in friction torque during acceleration.
- 6) When the discharge leakages of pump turbines increase in the future, there is the possibility of the

generator/motor rotating in the reverse direction of the pump. To prevent this, the brake release time was prolonged during the planning, but from the results of the maximum leakage test, it was evident that dynamic braking on the generator/motor side occurred and braking was also applied in the reverse direction. Thus it is possible to foresee a simplification of the brake control system in the future.

7) The simultaneous synchronous starting test of two generator/motor sets by one generator was conducted and we obtained excellent results as expected.

8) From the above points, the main constants were selected as follows: optimum excitation ratio:  $E_G/E_M = 1.35/0.86$  pu, guide vane opening speed: 0.56%/s, guide vane opening: 35%.

9) The effective operation of the protection devices, including a step-out detector to detect synchronous starting failure in the low frequency range was confirmed.

## II. THE SYNCHRONOUS STARTING METHOD

### 1. Features

The capacity of generator/motors for pumping-up power stations has greatly increased and is now in the 50 to 400 MVA range. Two kind of starting methods have been employed, one is a self-starting system in which the generator is started in the same manner as conventional induction motors and the other is a pony motor system directly coupled to the generator/motor. In the former case there are problems because of disturbances to the system in accordance with increase in the unit capacity and there were also limitations of the capacity because of the design of damper windings. In the latter case, there are few disturbances to the system. But since one starting motor is needed for each unit, so this is uneconomical and the efficiency is lowered in accordance with increased mechanical loss.

The synchronous starting method is a combination of the above two methods. There should be generator equipment to supply power for the motor in starting. Since this method has no direct connection to the system, there are no disturbances in the system.

One starting generator can be used to start several units simultaneously. Also, the generator capacity is only about 1/5 to 1/7 of the motor capacity when only one motor is started by the generator.

Since there are no disturbances to the system with this method it is most suitable for large capacity synchronous equipment like that used in pumping-up power stations. Two generators are provided in the Midono power station, and can be used as starting generators, therefore, the Midono station seems provide ideal conditions for use of the synchronous starting method.

## 2. Principles of the Synchronous Starting Method

The principles of this method are as shown in Fig. 1. The generator (*G*) which is directly coupled with turbine (*T*) is connected electrically to the generator/motor (*G/M*) which is directly coupled with the pump turbine (*P/T*). Both of these units excited, *G* is driven by water turbine *T* and current flows from *G* to *G/M*. *G/M* is then started by the synchronized torque which arises due to the interaction between the current and the flux on the *G/M* side. Reports of detailed analysis of this phenomenon have already been published.<sup>(1),(2)</sup> The two reaction theory was applied and simultaneous equations including nonlinear differential equations were derived by combining the electrical and mechanical systems. The results of calculations based on these equations using a computer and the results of actual tests performed on the testing machines were in good agreement. Therefore, this method was applied in planning this system and various characteristics were calculated. This article will not describe these theories again but the phenomena during the initial period of synchronous starting can be easily understood in terms of physics as follows. Assuming that from the time of *G/M* starting until synchronization is achieved, the generator speed *n*<sub>1</sub> does not change and *n*<sub>1</sub> is a constant very low speed, the electric torque *T*<sub>*e*</sub> which is transmitted to the motor side can be obtained from equation (1).

$$T_e = \frac{E_G \cdot E_M}{\sqrt{(R/n_1)^2 + x_d'^2}} \cdot \sin(\delta + \xi) - \frac{R/n_1(1-S)}{\{R/n_1(1-S)\}^2 + x_d'^2} \cdot E_M^2 \dots \dots \dots (1)$$

where *E*<sub>*G*</sub>, *E*<sub>*M*</sub>: Per unit excitation of *G* and *G/M*; the value necessary to produce no load rated voltage is

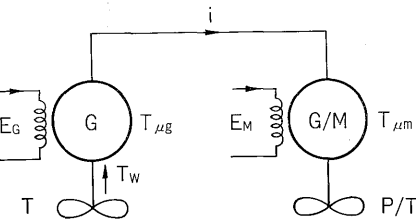


Fig. 1 Synchronous starting method

10 pu.

*R* = *R*<sub>*G*</sub> + *R*<sub>*G/M*</sub> + *R*<sub>*l*</sub>: The resistance of *G*, *G/M* and the bus line.

*x*'<sub>*d*</sub> = *x*'<sub>*dG*</sub> + *x*'<sub>*dM*</sub>: The transient reactances of *G* and *G/M*.

*δ*: The internal phase angle between *G* and *G/M*.

*S*: Slip

$$\xi = \tan^{-1} R/n_1 x_d'$$

1) The first item shows an acceleration torque *T*<sub>1</sub> which is transmitted from *G* to *G/M*. This torque is proportional to the product of *E*<sub>*G*</sub> and *E*<sub>*M*</sub> and is larger when the values of *R* and *x*'<sub>*d*</sub> are smaller. Since synchronization occurs when *n*<sub>1</sub> ≈ 0.01 to 0.03 pu and the frequency is very low, the influence of *R* is great. However, fortunately, in the large capacity units used in the pumping-up station when *G* and *G/M* are of the same capacity, *R* is usually not in excess of 0.01 pu and synchronization is easy to achieve.

2) Second item can be changed as follows

$$T_M = \left[ \frac{E_M}{\sqrt{(R/n_1(1-S))^2 + x_d'^2}} \right]^2 \cdot \frac{R}{n_1(1-S)} = I_M^2 \frac{R}{n_1(1-S)} \dots \dots \dots (2)$$

*T*<sub>*M*</sub> is the braking torque which arises because of the current *I*<sub>*M*</sub> which is caused to flow toward *G* by *E*<sub>*M*</sub> of the power with the series impedance *x*'<sub>*d*</sub> and *R/n*<sub>1</sub>(1-*S*) of the load. If *S* = 1, i.e. *G/M* is stopped, *T*<sub>*M*</sub> = 0 and if *S* = 0, i.e. synchronization has taken place, the impedance will be the same as that in the first item. With ∂*T*<sub>*M*</sub>/∂*n*<sub>1</sub> = 0, *n*<sub>1</sub> when *T*<sub>*M*</sub> is maximum can be obtained as follows.

$$n_{1m} = R/x_d'(1-S) \dots \dots \dots (3)$$

With *S* = 0, *n*<sub>1*m*</sub> ≈ 0.012 pu can be obtained when the actual machine data for this power station are substituted in the equation. In equation (1), it is assumed that sin(*δ* + *ξ*) = 1 and *S* = 0 and the actually measured constants are inserted. The results calculated for *n*<sub>1</sub> in this way are shown in Fig. 2. In order to transmit the torque from *G* to *G/M*, it is necessary that *G* is increased up to a certain speed. In Fig. 2, *T*<sub>1</sub> gradually increases as *n*<sub>1</sub> increases. *T*<sub>*M*</sub> reaches a maximum value when *n*<sub>1</sub> = 1.2%. The transmission torque *T*<sub>*e*</sub> = *T*<sub>1</sub> - *T*<sub>*M*</sub> is as shown in the figure. When *R* = 0.02 pu, the transmission torque *T*<sub>*e*</sub> is small as shown by the broken line in the figure 2. Therefore, it can be seen that *T*<sub>*e*</sub> is almost determined by three factors: *R*, *E*<sub>*G*</sub> and *E*<sub>*M*</sub>. The energy *F* transferred to the *G/M* side is

$$F = \int T_e d\rho$$

and if *F* is larger than the energy *F*<sub>*k*</sub> required for acceleration of *G/M* up to the speed *n*<sub>1</sub>, then synchronization is possible. If *F* is less than *F*<sub>*k*</sub>, synchronization is not possible. Therefore the limit at which synchronization is possible is when *F* is almost

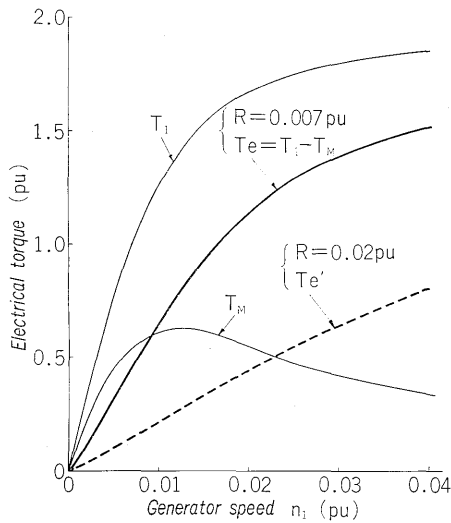


Fig. 2 Electrical torque vs. generator speed characteristics

equal to  $F_k$  and one of the aims of site test was to find out the characteristics of that limit.

3) When  $\partial T_e / \partial E_M = 0$  in equation (1), the relation between  $E_G$  and  $E_M$ , when the transfer torque is a maximum, can be obtained from equation (4).

$$\frac{E_G}{E_M} = \frac{2(R/n_1)}{\sqrt{(R/n_1)^2 + x_d'^2}} \cdot \frac{1}{\sin(\delta + \xi)} \quad (4)$$

$E_G \cdot E_M$  satisfying equation (4) is one of the condition in selecting the most optimum excitation ratio. Fig. 3 shows the relation between  $E_G/E_M$  and  $n_1$  when actually measured constants are substituted. The finally selected value of  $E_G \cdot E_M$  is also shown in Fig. 3. It is evident that this value is close to the value calculated from equation (4) when  $n_1$  is between 0.01 and 0.03.

### III. SPECIFICATIONS AND MAIN CIRCUITS OF THE EQUIPMENT

The specifications of the equipment used in this power station are as shown in Table 1. The main circuit is shown schematically in Fig. 4.

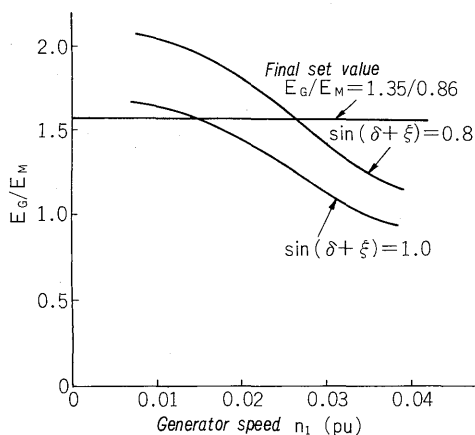


Fig. 3 Most suitable excitation ratio vs. generator speed characteristics

Table 1 Specifications of Tested Machines

	Item	Equipment for generating (G)	Equipment for pumping-up and generating (G/M)
Generator or generator/motor	Number of units	2	2
	Output (MVA)	65	65/63
	Speed (RPM)	167	150
	Voltage (kV)	11	11/10
	Frequency (Hz)	50	50
	Power factor	0.95	0.95/1.0
	GD <sup>2</sup> (t·m <sup>2</sup> )	6465	10283
	Direct axis synchronous reactance (pu)	0.954	0.903
	Quadrature axis synchronous reactance (pu)	0.67	0.596
	Stator winding resistance (Ω/phase at 75°C)	0.0076	0.00692
	No-load rated field current (A)	394	330/285
Directly coupled exciter	Output (kW)	330	350
	Voltage (V)	440	440
	Current (A)	750	796
Separate excitation equipment	Output (kW)	170	100
	Voltage (V)	240	220
	Current (A)	700	455
Water turbine or pump/turbine	Type	Francis turbine	Pump turbine
	Output (MW)	64.5	64/63
	Max. effective head or max. pumping head	80	80/81
	Discharge for generating or pumping (during pumping head) (m <sup>3</sup> /s)	90	90/63

### IV. PREPARATORY TESTS AND PLANNING

#### 1. Measurement of Circuit Resistance

The measured values of the resistance of  $G$  and  $G/M$  as well as of the starting bus line and the contact resistance of the circuit breaker and disconnecting switch are as shown in Table 2.

#### 2. Separate Excitation Equipment

It was planned that during synchronous starting, a constant exciting current should be supplied to  $G$  and  $G/M$  by separate excitation equipment up to about 80% of the rated speed. In order to ascertain the synchronous starting range and select the optimum value of  $E_G/E_M$ , separate excitation equipment for  $G$  and  $G/M$  were provided with taps as shown in Fig. 7, and confirmation tests of these taps and

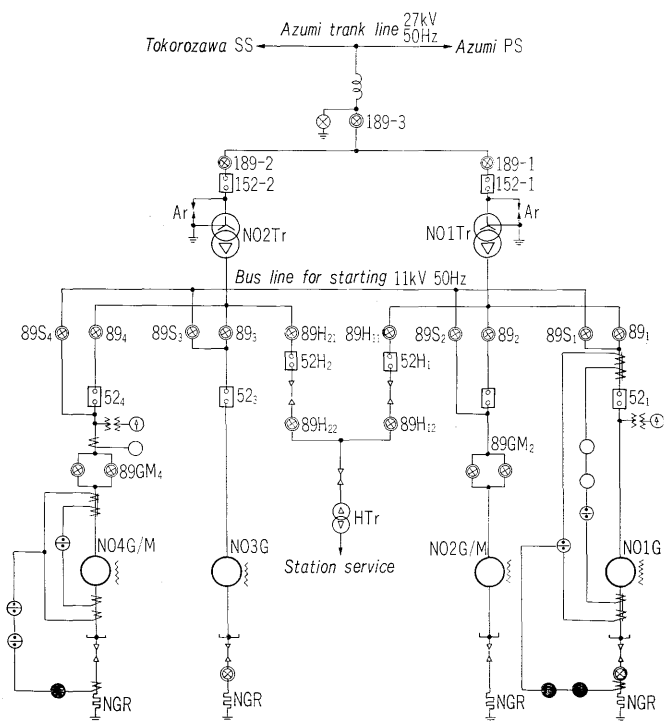


Fig. 4 Skeleton diagram of main circuit

Table 2 Measured Value of Resistance

	Mesured values of resistance pu (75°C)
Resistance of circuit $R_l$	0.0003
Resistance of G $R_G$	0.00415
Resistance of G/M $R_{G/M}$	0.00373
$R = R_l + R_G + R_{G/M}$	0.00818

exciting current were carried out. 1 pu of  $E_G$  and  $E_M$  is the exciting current required to produce the no load rated voltage of G and G/M. Fig. 5 shows a skeleton diagram of the excitation circuit.

### 3. Guide Vane Opening Speed Test

The guide vane opening speed (hereafter referred to as GVOS) is decided by considering various factors such as the starting time during synchronous starting, the turbine torque, the head, and 1G-1M and 1G-2M (the case when 2 generator/motors are started simultaneously with one generator). It was decided that 0.5 to 0.6%/sec is the best range, and it was planned to regulate GVOS approximately in this range. The results of the tests proved that the

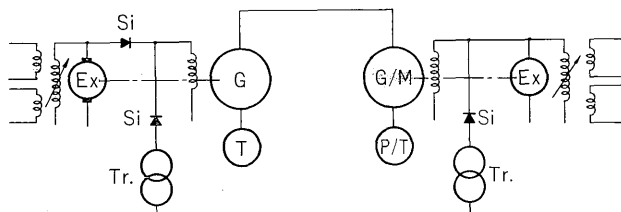


Fig. 5 Skeleton diagram of excitation circuit

value could be set freely between 0.2 and 1.0%/sec. From this result, a GVOS=0.56%/sec was employed in all subsequent synchronous starting tests.

### 4. Measurement of Maglager Characteristics of G, Static Friction Torque and Guide Vane Opening

In order to reduce the static friction torque in the generator during the initial period of synchronous starting, a Maglager device (a device which keeps the rotor raised by the electromagnet) is used<sup>(3)</sup>. The rotor suspension force is altered by controlling the exciting current in the Maglager device and in this way, it is possible to alter the static friction torque  $T_{\mu g}$  (i.e. the turbine starting torque  $T_{ws}$ ). In order to measure the turbine output torque  $T_w$ , a resistance wire strain gauge was placed in the turbine shaft and the torsional stress of the shaft (i.e. the turbine torque) was detected. This was then recorded on a magnetic oscillograph using telemeter equipment. Therefore, the turbine torque could be measured with high accuracy from rotating and through acceleration, and up to synchronization to the line.

The results of the test to determine the relation between Maglager exciting current  $I_{ml}$  and  $T_{\mu g} = T_{ws}$  are shown in Fig. 6. From this figure, it is evident that the value of  $T_{\mu g}$  can be set anywhere from 2 to 22% of the rated torque (380 t-m). The broken line in the same figure shows the relation between the guide vane opening and  $T_{\mu g}$ . Then we examine the relation between  $T_{\mu g}$  and the generator motor G/M static friction torque  $T_{\mu m}$ . When  $T_{\mu g}$  is less than  $T_{\mu m}$ , reliable synchronous starting is not possible especially for 1G-2M, but an oil lift system is employed on the G/M side, and  $T_{\mu m}$  is very small and  $T_{\mu g}$  is much greater than  $T_{\mu m}$ . In order that a certain

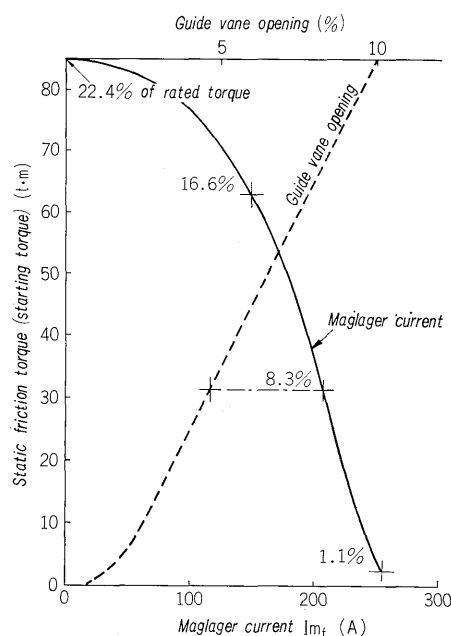


Fig. 6 Static friction torque vs. Maglager current, guide vane opening characteristics

torque is supplied by  $G$  at initial starting and  $G$  and  $G/M$  can be smoothly synchronized, it was originally planned that the starting torque  $T_{pg} = T_{ws}$  would be set at about 10%. For this, a Maglager current of 208 A was selected and  $T_{pg}$  was set at about 8%. The guide vane opening on start under these conditions was about 5%. The fact that  $T_{pg}$  can be selected freely in this way is an important feature of the Maglager system and is highly effective when the synchronous starting technique is used.

## 5. Measurement of Static Friction and Leakage Torques of G/M

### 1) Static friction torque

The results of measurement of the static friction torque by the action of the oil lift where  $G/M$  and  $P/T$  are coupled directly under conditions of no water in the penstock showed a very small value of  $T_{f.m} \cong 60 \text{ kg-m} = 0.00014 \text{ pu}$  (rated torque is 422 t-m).

### 2) Leakage torque

Considering the future leakage in  $P/T$ , the guide vane tightening was altered and the leakage torque  $T_l$  was measured. The torque during maximum leakage with  $G/M$  not excited when the gap of the guide vane teeth is 3.5 mm; generally the guide vane is repaired to have a less than 3.5 mm gap, was found to be about  $1.8 \text{ t-m} = 0.0043 \text{ pu}$ .

## 6. Test of Protective Relays in the Low Frequency Range

### 1) Short circuit fault and ground fault protection equipment during low frequency

When a complete short circuit occurs, an almost constant short circuit current flows which has no relation to the frequency. However, in the case of ground faults, the ground fault current should be considered as almost proportional to the frequency since the current is limited by a neutral grounding resistance. In static type relays consisting of transistors, frequency characteristics are very excellent. Therefore, this static type relay was used for protection against the above-mentioned faults in the low frequency range of  $G$ . Site tests were conducted on these relays and it was confirmed that the operating point of the relays were flat in the 10 to 50 Hz range.

### 2) Step-out detection equipment

A gear-shaped circular plate is attached to the main shaft of both  $G$  and  $G/M$ . Proximity switches are provided opposite this plate. The output pulses of the switches are extracted and whether or not there will be step-out of the  $G$  and  $G/M$  is decided by a transistor circuit. Electrical angle differences of  $180^\circ$  or more are detected.

## 7. Switching Test of Excitation Equipment

At 80% of the rated speed of  $G$ , excitation of  $G$  is switched from the separate excitation equipment to the direct-coupled exciter and AVR is switched on. The bus line voltage is then maintained at the

planned value. Next,  $G/M$  excitation is switched from the separate excitation equipment to the direct-coupled exciter and APFR is switched on. The above switching method is reliable and stable. As can be seen from the oscillogram in Fig. 16, the time from when AVR is switched on at about 80% of the rated speed up to the time AVR operation is completed, is only about 3 sec. This is due to the fact that silicon rectifier for block of reverse current patented by Fuji Electric is provided in the exciting circuit and equipment consisting of thyristor which controls the exciter field is employed.

## V. SYNCHRONOUS STARTING TEST (STARTING IN AIR)

Synchronous starting tests were performed when the water level was depressed below the runner by air of the air tank and air compressor in the pump turbine. The tests are divided into three important parts including the problems of initial synchronization, acceleration and switching.

### 1. Test to Confirm Initial Synchronous Starting Range

The possibility of synchronization of  $G/M$  with  $G$  during initial starting, is a very important point in the synchronous starting system. As described in section II, various parameters exert influence but it is easy to decide the possible synchronization range from the plot method with a profile of  $E_G - E_M$ . Therefore,  $GVOS = 0.56\%/sec.$  and Maglager current of 208 A were set.  $E_G$  and  $E_M$  were varied and the rotational speed of  $G$  was sped up to about 20% of the rated speed. The possibility or impossibility of synchronization was tested.

From the results, the V curve was obtained and is shown as curve (I) Fig. 7. The symbols used in this figure have meanings as follows.

- : Synchronous starting is possible up to 20% of the rated speed
- Δ: Synchronous starting is possible up to 20% of the rated speed but hunting occurs at the time of synchronization
- ×: Synchronization is not possible
- ⊙: Synchronization and acceleration is possible up to 100% of the rated speed
- ⊗: Synchronization is possible up to 20% of the rated speed but when accelerated to 100% of the rated speed, step-out occurred.
- : Synchronization up to 100% of the rated speed is possible when the pump turbine runner is in water.
- : Step-out occurred when the speed was accelerated to 100% when the pump turbine runner is in water.

Fig. 8 shows oscillograph No. 14 in which the point of  $E_G \cdot E_M = 0.561/0.50 \text{ pu}$  is comparatively far from the V curve of Fig. 7. Fig. 9 shows oscillograph No. 12 in which the  $E_G/E_M = 0.748/1.41 \text{ pu}$ . The values are shown by the Δ marks in Fig. 7 which show possible

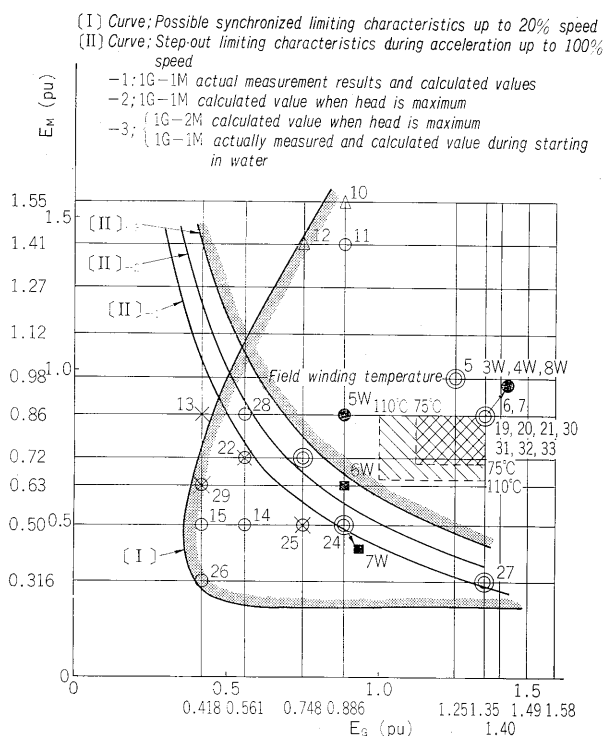


Fig. 7 Characteristics of limiting curves for synchronous starting

synchronization limits nearer the  $V$  curve. In this case, for about 30 seconds after starting of  $G$ , bus line current fluctuation occur and synchronization gradually becomes possible. Fig. 10 shows oscillogram No. 13 in which the  $E_G/E_M=0.418/0.86$  pu. This is equivalent to the  $\times$  marks in Fig. 7 when synchronization is not possible.

As described in a previous paper<sup>(2)</sup>, the  $V$  curve

was obtained by means of a computer. The overall resistance was to be  $R=0.00883$  pu (at  $75^\circ\text{C}$ ) in the original plan but since the stator winding temperature was  $36^\circ\text{C}$  on the  $G$  side,  $25^\circ\text{C}$  on the  $G/M$  side and  $20^\circ\text{C}$  on the bus line side during tests, the resistance was fixed at  $R\approx 0.007$  pu, only about 80% of the planned value. Therefore, the possible starting range could be somewhat larger than that originally planned. When calculations were again made with the computer by substituting various values obtained from the site tests, it was reconfirmed that the values calculated by the computer could be used for the synchronization possible range for synchronous starting since the two sets of values were in close agreement.

## 2. 100 % Speed Acceleration Test

### 1) Test to confirm the possible starting range

After  $G/M$  has been synchronized with  $G$ , the speed is accelerated to the rated speed but the acceleration time is dependent on the turbine torque  $T_w$  coupled to  $G$  and the electrical characteristics appear to resemble the problem concerning the transmission of the power between two machines in the power system.

First, concerning turbine torque control, the guide vane opening (GVO), which is a parameter for the turbine torque/speed characteristics curves as shown in Fig. 11, is set at 35% for example and when the guide vane is opened at a constant speed up to this value, the turbine torque  $T_w$  can be shown approximately by equation (5).

$$T_w = (K_1 \cdot \alpha \cdot t - K_2 \cdot n / \sqrt{H}) \cdot H \text{ (pu)} \dots \dots \dots (5)$$

where  $\alpha$ : Guide vane opening speed (GVOS)  
 $H$ : Effective head 68.2 m = 1 pu  
 $n$ : Speed pu

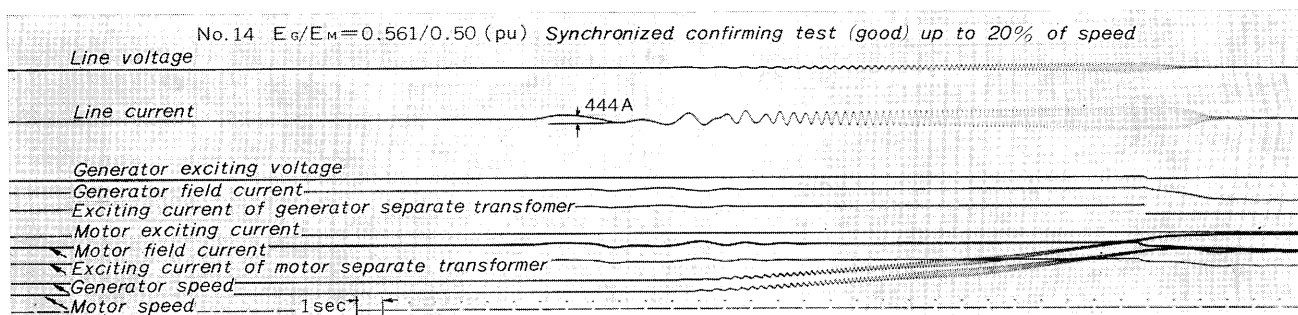


Fig. 8 Confirming test of synchronized phenomena (good)

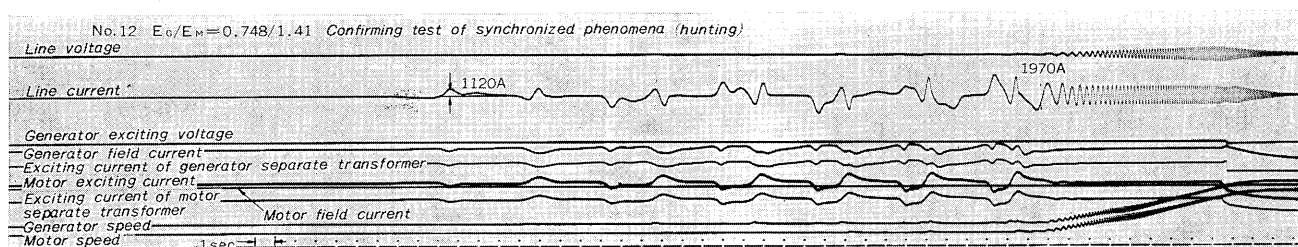


Fig. 9 Confirming test of synchronized phenomena (hunting)

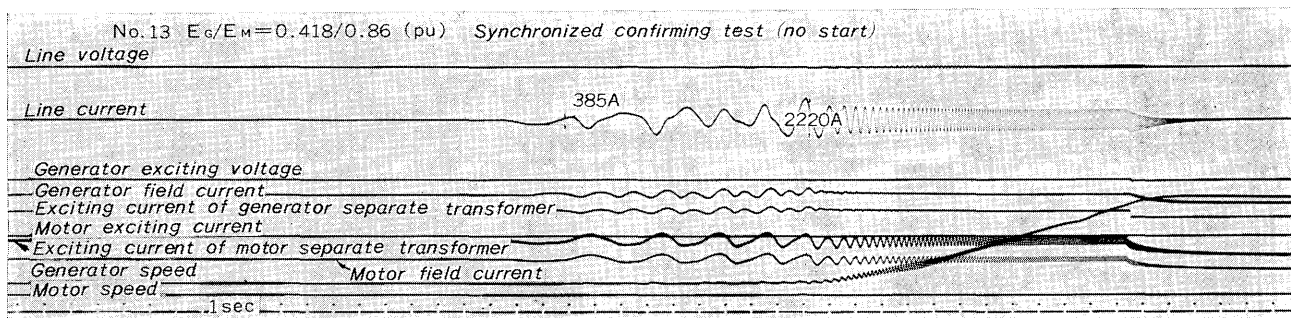
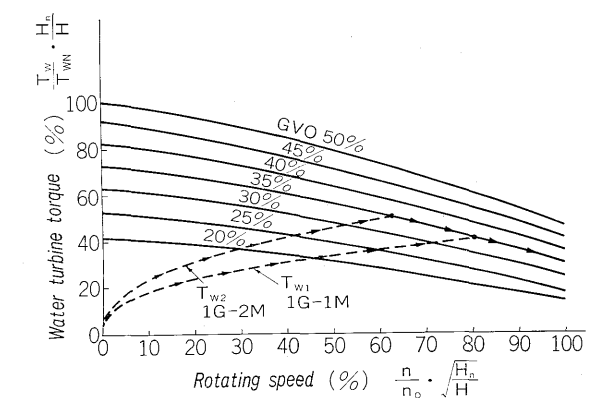


Fig. 10 Confirming test of synchronized phenomena (no starting)



$T_{WN}=380 \text{ t}\cdot\text{m}$   
 $T_W$ : Turbine torque  
 $n_0=167 \text{ rpm}$   
 $n$ : Rotating speed  
 $T_{W1}$ : G/M synchronous starting of one unit  
 $T_{W2}$ : G/M synchronous starting of two units simultaneously  
 $H_n=68.2 \text{ m}$   
 $H$ : Effective head  
 $\text{GVO}$ : Guide vane opening  
 $\text{GVOS}=0.56\%/ \text{sec}$

Fig. 11 Water turbine torque vs. speed characteristics (calculated value)

$K_1$  and  $K_2$ : Constants

Since  $G$  and  $G/M$  are already synchronized, the remaining torque of  $T_W - T_{lg} - T_{lm}$  is used for acceleration of  $G$  and  $G/M$ . The distribution of this torque is as shown in equation (6) since it is proportional to the acceleration constants.

$$T_W - (T_{lg} + x \cdot T_{lm}) = (T_{jG} + x \cdot T_{jM}) \frac{dn}{dt} \quad (6)$$

where  $T_{lg}$  and  $T_{lm}$ : The friction torque of  $G$  and  $G/M$  respectively. (loss torque of mechanical loss, iron loss etc.)

$T_{jG}$  and  $T_{jM}$ : The acceleration constants of  $G$  and  $G/M$ , 7.6 and 9.8 sec. respectively.

$x$ : Number of units of  $G/M$  which are simultaneously started.

It calculations are made from equations (5) and (6) using a computer, the turbine torque characteristics are as shown by the broken lines in Fig. 11 for  $1G-2M$  and  $1G-1M$ .

The torque which should be transmitted from  $G$  to  $G/M$ , i.e.  $T_W - T_{lg}$  is transmitted by the electrical torque  $T_e$  between the two units. Fig. 12 shows a vector diagram of the synchronous torque during

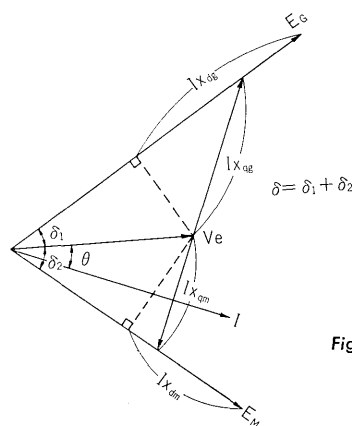


Fig. 12 Vector diagram in high speed range

acceleration. If the reaction torque is neglected,  $T_e$  can be expressed as in equation (7).

$$T_e = \frac{E_G \cdot E_M}{(x_{dg} + |x \cdot x_{dm}|)} \sin(\delta_1 + \delta_2) \quad (7)$$

where  $x_{dg}$  and  $x_{dm}$ : synchronous reactance of  $G$  and  $G/M$ . One of the conditions necessary to prevent step-out during acceleration is that  $T_e$  is generally larger than  $T_W - T_{lg}$ . The torque transmitted to  $G/M$  can be expressed by equation (8).

$$T_m = [x T_{jM} / (T_{jG} + x T_{jM})] \cdot T_W \quad (8)$$

Therefore, resolving equation (7) and (8) under the condition that  $T_e > T_m$ , equation (9) can be obtained.

$$E_G \cdot E_M > \frac{T_{jG} + x \cdot T_{jM}}{x \cdot T_{jM}} \cdot \frac{(x_{dg} + |x \cdot x_{dm}|)}{\sin(\delta_1 + \delta_2)} \cdot T_W \simeq K \cdot T_W \quad (9)$$

Equation (9) means that  $T_W$  is determined, the minimum value of the excitation product of  $E_G$  and  $E_M$  can be determined.  $T_W$  is determined by GVOS and GVO. When GVO is set at 35% and the relation between GVOS and the minimum value of  $E_G \cdot E_M$  is calculated by a computer, Fig. 13 and Fig. 14 for  $1G-2M$  and  $1G-1M$  respectively are obtained with the head as parameters.

In the site tests, the relation between the measured value of  $T_W$  during acceleration and the excitation product, i.e. the step-out limit characteristics were determined and serve as data for selection of the optimum excitation ratio. Acceleration was carried out at  $\text{GVO}=35\%$  and  $\text{GVOS}=0.56\%/ \text{sec}$  and it

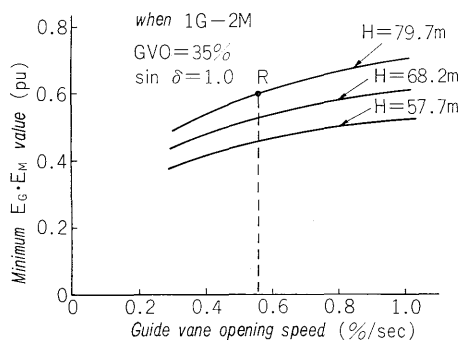


Fig. 13 Minimum  $E_G \cdot E_M$  vs. GVOS characteristics (1G-1M)

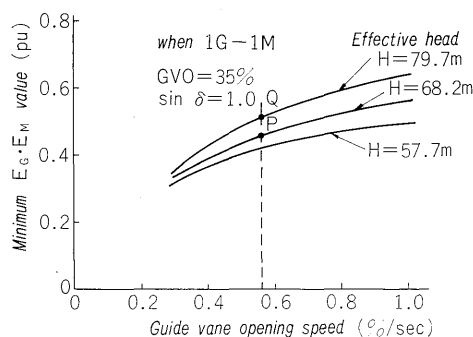


Fig. 14 Minimum  $E_G \cdot E_M$  vs. GVOS characteristics (1G-2M)

was investigated whether or not synchronization was maintained up to 100% of the speed. In the possible starting ranges shown in Fig. 7, the  $\otimes$  marks indicate that synchronization was possible up to 20% of the speed but if the speed was increased to 100%, step-out occurred at some point. The  $\odot$  marks show points where synchronization was possible up to 100% of the speed and therefore the limit characteristics are like curve II-1. These characteristics can be shown by a hyperbolic function as indicated in equation (9). The area to the right side of this curve is the possible starting region. When compared with the planned values in Fig. 13, the head during the tests was equivalent to approximately the standard head and therefore point P in Fig. 13 where  $E_G \cdot E_M = 0.45$  showed that the test result  $E_G \cdot E_M = 0.43$  which is very good agreement. An example of the  $\otimes$  marks is shown in oscillograph No. 29 in Fig. 15. In this figure, at the excitation ratio of  $E_G/E_M = 0.418/0.63$  pu,  $E_G \cdot E_M$  was only 0.256 and therefore the G/M

stepped-out at 45 rpm or 27% of the rated speed. Operation of step-out detection relay #56 causes the exciting circuits of both units to be switched off.

The bus line current is therefore attenuated at the transient short circuit time constant  $T_d'$ , which is determined as connected the load. Since the test were conducted with a standard head, the excitation product  $E_G \cdot E_M$  becomes 0.5 pu from point Q in Fig. 13, assuming the maximum effective head 79.7 m in case of 1G-1M.

Therefore, this gives curves II-2 shown in Fig. 7. In the case of 1G-2M with maximum head  $E_G \cdot E_M$  is 0.59 from point R in Fig. 14 which means curve II-3 in Fig. 7. Therefore excitation for G and G/M must be selected in the right hand region limited by the II-3 curve as the limit conditions for maximum head with 1G-2M and the I curve for possible initial synchronization. Then we conducted synchronous starting tests on 1G-2M, the oscillogram of one of which is shown in Fig. 17. Test results proved that the curve II-3 in Fig. 7 was correct.

## 2) Selection of excitation ratio

Besides considering the possible starting range as described in section 1), the temperature variation of the field windings of both units between 20°C and 110°C must be considered when determining the most preferable excitation ratio.

Considering also that the starting current is small and starting is stable, the excitation for both units was set as follows with GVOS = 0.56 %/s, and GVO = 35%.

$$\begin{aligned} E_G &= 1.35 \text{ pu} \\ E_M &= 0.86 \text{ pu} \end{aligned}$$

Fig. 16 shows an oscillogram of a test from starting to synchronization to the line at these final taps. It is evident that there is smooth operation in each part from the time the excitation circuit is switched on until the time the separate excitation equipment is switched off. The bus line current is only 35% of the rating at a maximum. Part (b) of Fig. 16 shows the  $T_w$  of the turbine on the G side, GVO, the starting mark and operation of the interrupter. In 8.8 sec. after the guide vane starts to open, the guide vane opening reaches 5.5% and the machine begins to rotate. The relation between  $T_w$ , GVO and the starting time is shown in Fig. 18. From this figure

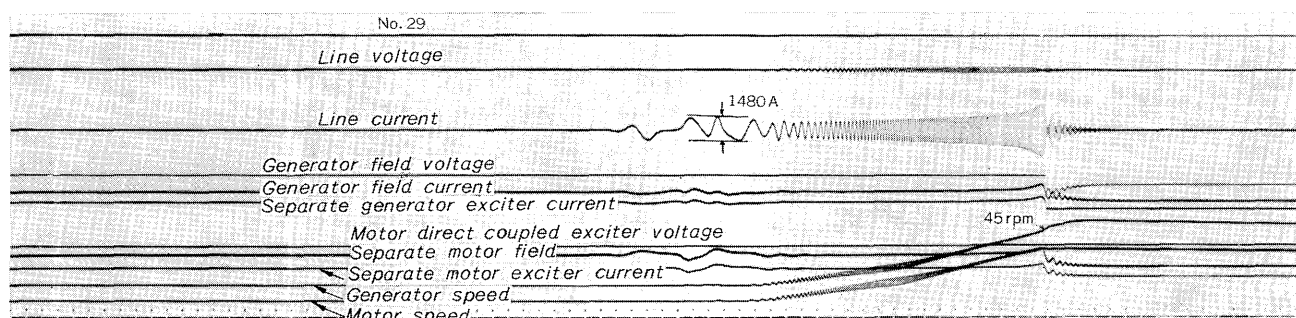


Fig. 15 Step-out phenomena at high speed region



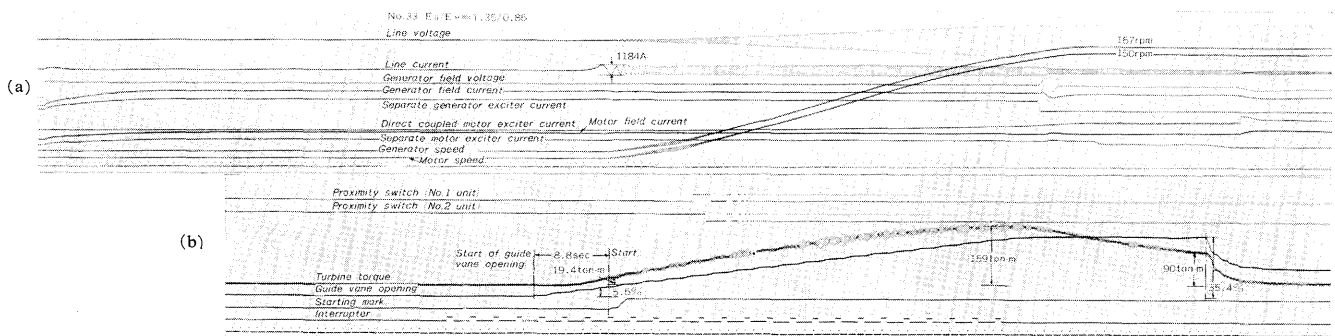


Fig. 16 Synchronous starting up to parallel running (1G-1M)

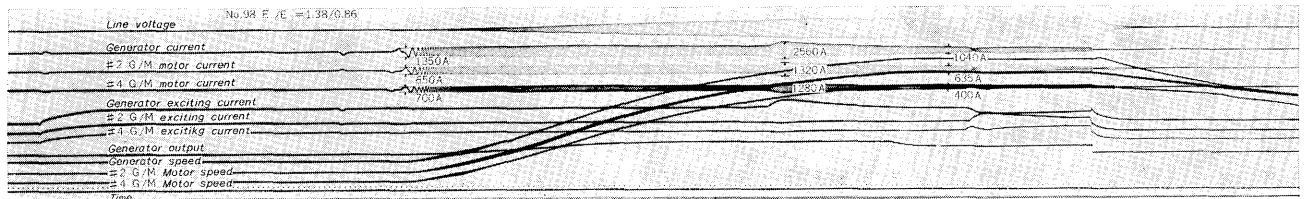


Fig. 17 Synchronous starting test to parallel running (1G-2M)

$T_w$  can be seen to agree well with the characteristics in Fig. 11, and it indicates that the calculations are highly reliable.

### 3) Acceleration time

Fig. 19 shows the acceleration time characteristics during synchronous starting. From the time of the main circuit CS#1 ON until synchronization to the line requires 4 minutes and 53 seconds, but the acceleration time from the time  $G$  has started to rotate up to the time 100% of the rated speed is reached is only 58 seconds. Test results when the GVO was changed to 25% showed that the acceleration time was prolonged for only 3.5 sec. when compared with the 35% GVO. Since the 1G-1M tests were carried out using the standard head, investigations were made at other conditions. Fig. 20 shows calculated values of the acceleration time in respect to the GVOS with the head and number of units as parameters. The following is with a GVOS of 0.56%/sec.

- 1) Even if the head is a minimum of 57.7 m for 1G-1M, the acceleration time increases by only 10 seconds when compared with the time of the standard head.
- 2) At the standard head for 1G-2M, the acceleration time was assumed to be 90 seconds and test results

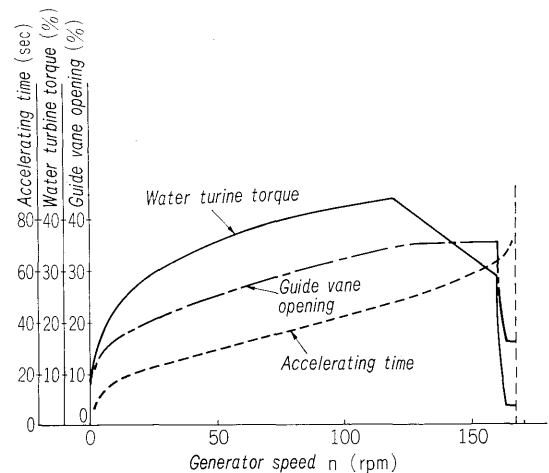


Fig. 18 Measured values of turbine torque, guide vane opening and acceleration time

showed good agreement. This value is increased only by about 20 seconds at the minimum head. Therefore we concluded that during planning, the values of  $E_G/E_M$ , GVOS and GVO must be fixed constant and controlled for both 1G-1M and 1G-2M no matter how the head varies. Simplification of system control and easy starting were attained. These were expected

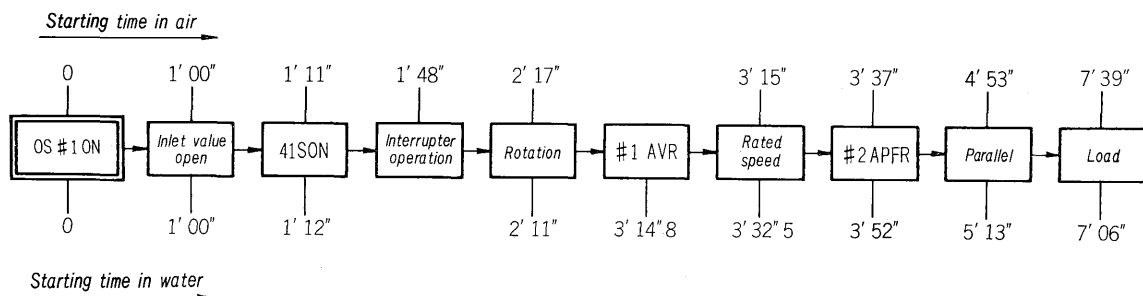


Fig. 19 Starting time characteristics

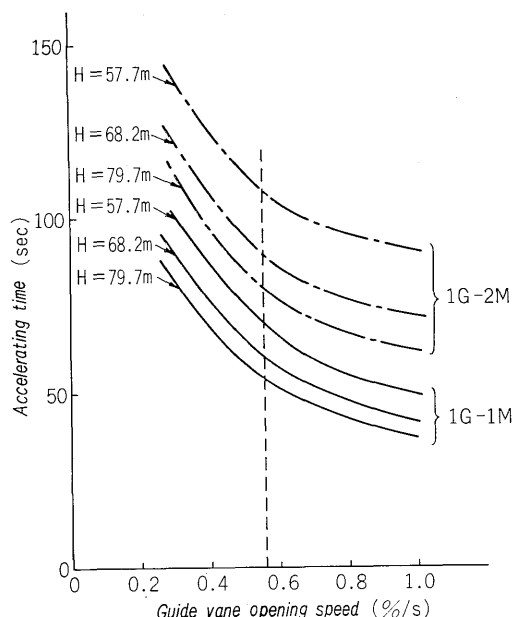


Fig. 20 Accelerating time vs. guide vane opening speed characteristics

during planning.

### 3. Excitation Switching and Synchronization Tests

As can be seen from Fig. 16, excitation of *G* is switched at 80% of the speed and about 3 seconds after AVR operation is completed smooth. For *G/M*, APFR operation is completed in 22 seconds after the speed reaches 100% and synchronization to the line was made in 1 minute and 16 seconds after the automatic synchronizing equipment of the *G* began to operate. At this moment, *G* is cut off and *G/M* starts filling the runner chamber with water and opening the guide vane. Then pumping operation begins.

## VI. SYNCHRONOUS STARTING TEST (IN WATER)

A synchronous starting test in water was performed without using water level depression equipment for the pump turbine to check for some problems. The method and aim of the test were as follows. The guide vane opening was changed from 35% to 55% considering the increase of the friction torque. The possible starting region during acceleration and whether actual starting was possible or not were confirmed. Checks were made concerning the water pressure, temperature, and vibration in each part of

pump turbine during operation as well as runner loss in water.

1) As the problem of synchronization during initial starting was the same as that of starting in air, test were performed to find the step-out limit characteristics up to 100% speed. The results obtained were between test No. 5W and 7W as shown in Fig. 7. The  $E_G \cdot E_M$  limit characteristics were the same as for curve II-3 in Fig. 7. For starting in water, the runner friction torque increases sharply when the speed is increased and this means that the torque which should be transmitted from *G* to *G/M* should also increase. Equation (10) is equivalent to equation (9) for 1G-1M.

$$E_G \cdot E_M > \frac{T_{jM}}{T_{jG} + T_{jM}} \cdot \frac{(x_{dg} + x_{dm})}{\sin(\delta_1 + \delta_2)} \cdot T_w \cdot \left(1 + \frac{T_{jG}}{T_{jM}} \cdot \frac{T_L}{T_w}\right) \dots\dots\dots (10)$$

When the value of  $T_L$  actually measured in the tests as  $\approx 17,000$  kW is substituted in the above equation,  $E_G \cdot E_M \approx 0.6$  pu is obtained which is almost the same as curve II-3 in Fig. 7. With the  $E_G/E_M$  fixed at 0.886/0.5 pu of 7W in Fig. 7, step-out occurred at 75% of the speed and the oscillogram is as shown in Fig. 21.

2) The time required up to 100% speed from the starting of *G* is 82 seconds. This means that 24 seconds or more are required than 58 seconds for starting in air but the time from CS#1 closing until synchronization to the line is 5 minutes and 13 seconds in water and 4 minutes and 53 seconds in air. Since the portion for the increase in acceleration time is larger than that for the reduction of time for water level depression in the case of starting in water, starting in water on the whole is about 20 seconds longer. Fig. 22 shows an oscillogram from starting until parallel pumping.

3) Vibrations in the pump turbine are reduced rapidly when the guide vane begins to open after synchronization to the line although they begin to increase from the speed where the priming water pressure is established (86%). Therefore, precautions must be taken because the vibrations during this period and the water pressure are larger than when starting in air. However, in the previous pony motor and self-starting systems, starting in water was not desirable because of the large friction torque but with the synchronous starting system it is possible. Therefore, these tests provided valuable data for the

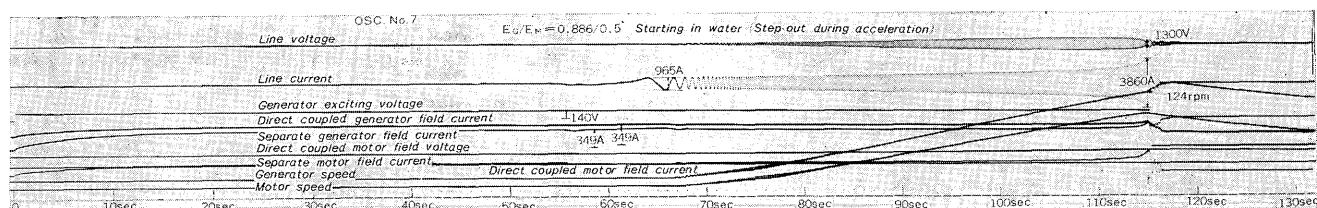


Fig. 21 Step-out phenomena at high speeds with runner in water

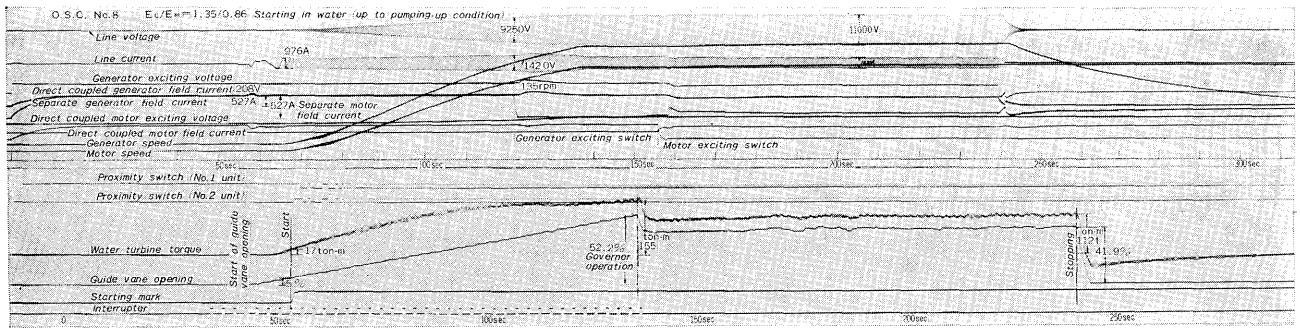


Fig. 22 Synchronous starting test to pumping-up condition with runner in water

construction of future pumping up power stations concerning with the reliability of starting in water and whether or not water level depression equipment is used.

## VII. SYNCHRONOUS STARTING DURING MAXIMUM LEAKAGE

In order to investigate the influence on synchronous starting when the leakage of the pump turbine reaches a maximum value in the future, the guide vane tightening was set at the maximum leakage value and a test was performed. The biggest problem when the leakage increases is that  $G/M$  will rotate in the reverse direction of the pump and there will be a speed difference greater than the possible synchronous starting speed difference between the two units (0 to 3%) and synchronization will become impossible. However, the test results show that because of the dynamic braking torque when  $G/M$  operates (as shown in equation (11)), the speed of  $G/M$  drops by only the very small value of 0.01 rpm (0.0067%) and there is therefore no problem concerning synchronization.

$$T_B(n) = \frac{R[R^2 + n^2 \cdot X_q^2] \cdot n}{[R^2 + n^2 \cdot X_d \cdot X_q]^2} \cdot E_M^2(\text{pu}) \quad \dots\dots (11)$$

where  $R$ : Same as for equation (1)  
 $n$ : Rotating speed (pu)

$X_d \simeq X_{dm} + (X_{dg} + X_{qg})/2$ :  
 Direct axis synchronous reactance viewed from  $G/M$  side

$X_q \simeq X_{qm} + (X_{dg} + X_{qg})/2$ :  
 Quadrature axis synchronous reactance viewed from  $G/M$  side

As shown in Fig. 23, when the maximum leakage torque  $T_L$  is 1.8 t-m, the dynamic braking torque  $T_B$  as shown in equation (11) is 1 t-m or more. Therefore, the rotating torque in respect to  $G/M$ ,  $T_L - T_B$ , is very small. A similar test was conducted for 1G-2M in which the leakage of one  $G/M$  was minimum and the other maximum. In a few seconds

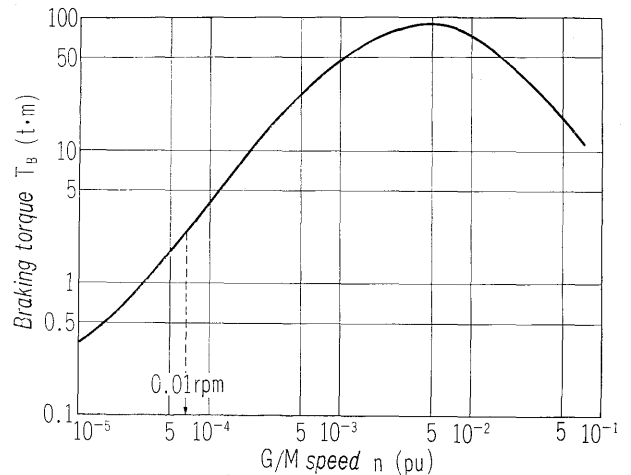


Fig. 23 Dynamic braking torque speed characteristics of  $G/M$

after applying excitation,  $G/M$  rotation in reverse direction stopped, and 2 sets of  $G/M$  could start simultaneously.

## XIII. CONCLUSION

The synchronous starting site tests conducted at the Midono power station are the first of their type in the world. As the planning, manufacturing and tests adopted the latest techniques the test results were as good as expected. The results of these tests will probably lead to the adoption of the synchronous starting method not only in this power station but also in large capacity pumping-up stations in the future. Finally the authors wish to thank all those who participated in this work and especially Mr. Ikeda of the Tokyo Electric Power Co. for cooperation in the site tests.

## References:

- (1) Nakata, Mi. Takahashi: Joint Conference of the Institute of Electrical Engineer of Japan (1965)
- (2) Nakata, Mi. Takahashi: Fuji Elect. J. 38 No. 7 (1965)
- (3) Ma. Takahashi, Mi. Takahashi, Kambara: Fuji Elect. J. 42 No. 11 (1969)
- (4) Kambara, Inoue: Fuji Elect. J. 43 No. 3 (1970)